Electronic Supplementary Information for

The linear relationship derived from deposition potential of Pb-Ln alloy and atomic radius

Hengbin Xu,[a] Jiamiao Qu,[a] Milin Zhang,[a,b*] Yongde Yan,[a] Xin Sun,[a] Yanghai Zheng,[a] Min Qiu[b] and Li Liu[b]

[a]*Key Laboratory of Superlight Materials and Surface Technology, Ministry of Education, College of Materials Science and Chemical Engineering, Harbin Engineering University, Harbin 150001, China*

[b]*College of Science, Heihe University, Heihe 164300, China*

Corresponding author: Milin Zhang

Telephone: +86-451-82569890

E-mail address: zhangmilin@hrbeu.edu.cn

SI.1 The details of the preparation and purification of the melt

The temperature of melts was measured with a nickel chromium-nickel aluminium thermocouple sheathed with an alumina tube. Rare earth ions were introduced into the bath in the form of dehydrated $ReCl_3$ powder (99.9%, analytical grade; Sinopharm Chemical Reagent Co. Ltd). To prevent the formation of ReOCl in melts, before each experiment, HCl was bubbled into the melt for 30 min to remove oxide ions. Then Ar gas was bubbled into the melt to remove residual HCl, oxygen and water; the oxygen content and moisture levels were maintained below 1 ppm. All electrochemical experiments were done in a purified eutectic mixture under an inert argon atmosphere to control the temperature of the furnace to ±2 K. The working temperatures were measured with a nickel-chromium thermocouple.

The details of preparation of electrochemical apparatus and electrodes

All electrochemical measurements (involving cyclic voltammetry, square wave voltammetry and open circuit chronopotentiometry) were employed using an Autolab PGSTAT 302N (Metrohm, Ltd) with Nova 1.8 software package. A silver wire (d = 1 mm, 99.99% purity) dipped into a solution of AgCl (1.0 wt.%) in LiCl-KCl (63.8:36.2

mol%) eutectic melts contained in 3 mm diameter quartz tube was used as the reference electrode. All potentials were referred to this Ag/Ag^+ couple. The bottom of the alundum tube was polished to be very thin and used as a diaphragm. A spectral pure graphite rod (d = 6 mm) served as the counter electrode. The working electrodes were molybdenum wires (d = 1 mm, 99.99% purity). The lower end of the molybdenum wires was polished thoroughly using SiC paper, then cleaned ultrasonically with dilute hydrochloric acid and ethanol prior to use. Between each measurement working electrodes were cleaned by applying an anodic polarization. The active electrode surface area was determined after each experiment by measuring the immersion depth of the electrode in the molten salts.

SI.2 For assigning the attribution of the redox peaks and identify the real reaction, we compared these peak potentials (CV, SWV and OCP) to determine the real reaction

For example: The following reaction occurs in SWV.

Peak A: $Li(I) + e^- \not\rightleftharpoons Li(0)$

Peak B, C, D, E: $X\ Pb(II) + Y\ Li(I) \not\rightleftharpoons Pb_xLi_y$

Peak F: $Gd(III) + 3e^- \not\rightleftharpoons Gd(0)$

Peak I: $X\ Gd(III) + Y\ Pb(II) \not\rightleftharpoons Gd_xPb_y$

Peak G: $Pb(II) + 2e^- \not\rightleftharpoons Pb(0)$

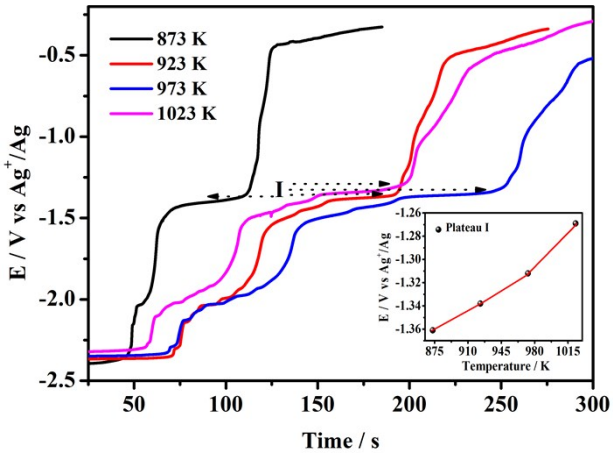

Fig. S1 Open circuit chronopotentiometry curves at Mo electrodes (S = 0.332 cm^2) of the LiCl-KCl-$PbCl_2$ (2.0 wt.%)-$GdCl_3$ (2.0 wt.%) molten salts systems, after deposition at -2.5 V for 10 s,

at different temperatures. Inset: plots of potentials for plateau I at different temperatures.

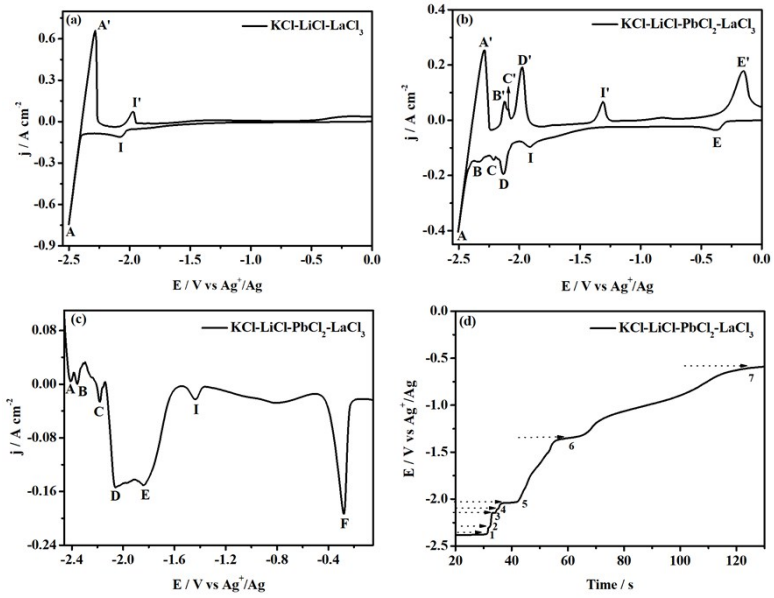

Fig. S2 (a) CV obtained in LiCl-KCl after addition of $LaCl_3$ (2.0 wt.%) on Mo electrode at 0.1 V/s. (b) CV obtained in LiCl-KCl after addition of $PbCl_2$ (2.0 wt.%) and $LaCl_3$ (2.0 wt.%) on Mo electrode at 0.1 V/s. (c) SWV of the LiCl-KCl melts after the addition of $PbCl_2$ (2.0 wt.%) and $LaCl_3$ (2.0 wt.%) on Mo electrode. Pulse height: 25 mV, Potential step: 1 mV, Frequency: 20 Hz. (d) OCP curves obtained on Mo electrode after potentiostatic electrolysis at -2.5 V (vs Ag/Ag^+) for 10 s in LiCl-KCl-$PbCl_2$ (2.0 wt.%)-$LaCl_3$ (2.0 wt.%) melt. Temperature: 873 K

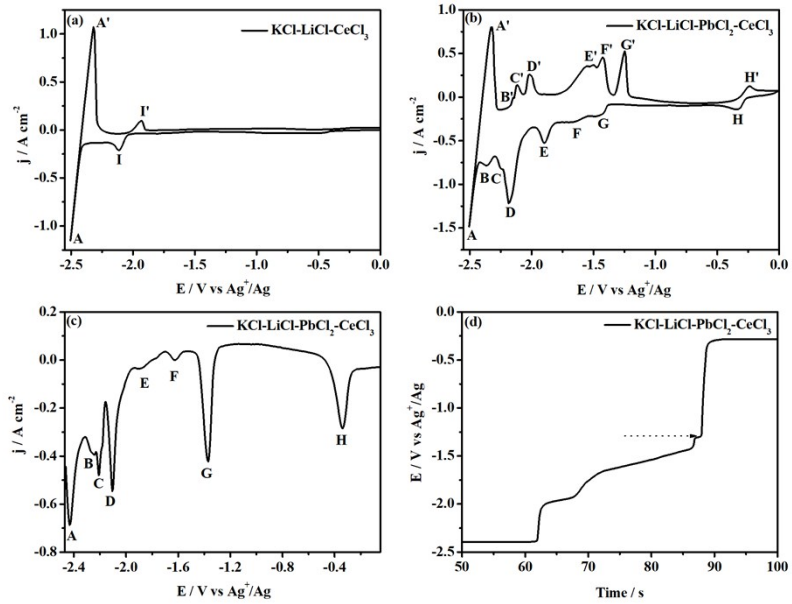

Fig. S3 (a) CV obtained in LiCl-KCl after addition of $CeCl_3$ (2.0 wt.%) on Mo electrode at 0.1 V/s. (b) CV obtained in LiCl-KCl after addition of $PbCl_2$ (2.0 wt.%) and $CeCl_3$ (2.0 wt.%) on Mo electrode at 0.1 V/s. (c) SWV of the LiCl-KCl melts after the addition of $PbCl_2$ (2.0 wt.%) and $CeCl_3$ (2.0 wt.%) on Mo electrode. Pulse height: 25 mV, Potential step: 1 mV, Frequency: 20 Hz. (d) OCP curves obtained on Mo electrode after potentiostatic electrolysis at -2.5 V (vs Ag/Ag^+) for 10 s in LiCl-KCl-$PbCl_2$ (2.0 wt.%)-$CeCl_3$ (2.0 wt.%) melt. Temperature: 873 K

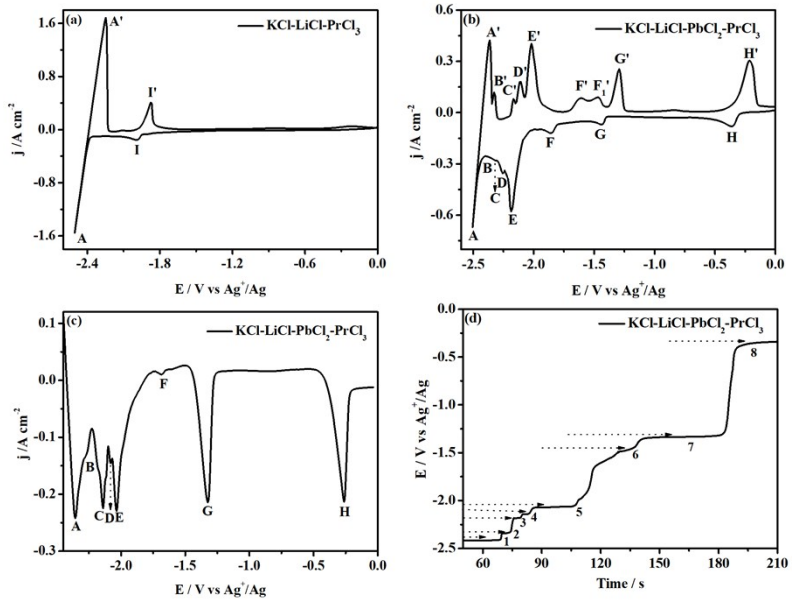

Fig. S4 (a) CV obtained in LiCl-KCl after addition of $PrCl_3$ (2.0 wt.%) on Mo electrode at 0.1 V/s. (b) CV obtained in LiCl-KCl after addition of $PbCl_2$ (2.0 wt.%) and $PrCl_3$ (2.0 wt.%) on Mo electrode at 0.1 V/s. (c) SWV of the LiCl-KCl melts after the addition of $PbCl_2$ (2.0 wt.%) and $PrCl_3$ (2.0 wt.%) on Mo electrode. Pulse height: 25 mV, Potential step: 1 mV, Frequency: 20 Hz. (d) OCP curves obtained on Mo electrode after potentiostatic electrolysis at -2.5 V (vs Ag/Ag^+) for 10 s in LiCl-KCl-$PbCl_2$ (2.0 wt.%)-$PrCl_3$ (2.0 wt.%) melt. Temperature: 873 K

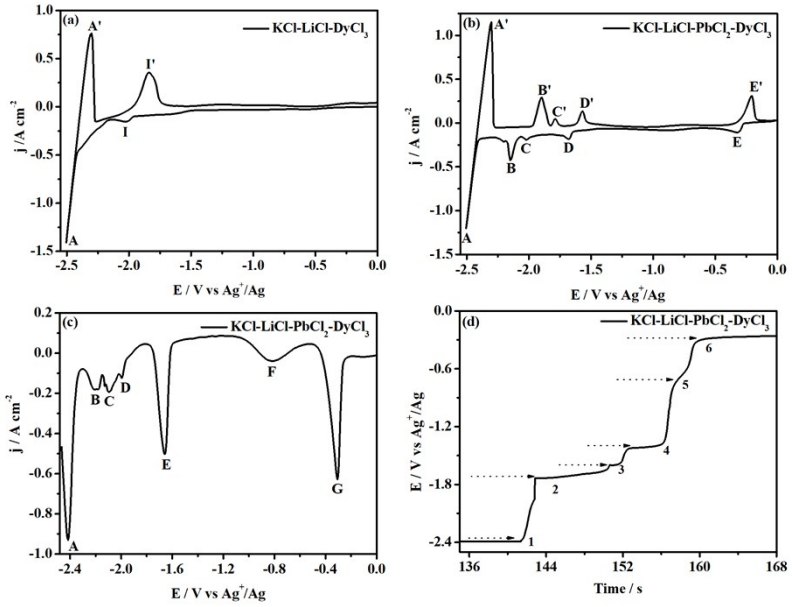

Fig. S5 (a) CV obtained in LiCl-KCl after addition of $DyCl_3$ (2.0 wt.%) on Mo electrode at 0.1 V/s. (b) CV obtained in LiCl-KCl after addition of $PbCl_2$ (2.0 wt.%) and $DyCl_3$ (2.0 wt.%) on Mo electrode at 0.1 V/s. (c) SWV of the LiCl-KCl melts after the addition of $PbCl_2$ (2.0 wt.%) and $DyCl_3$ (2.0 wt.%) on Mo electrode. Pulse height: 25 mV, Potential step: 1 mV, Frequency: 20 Hz. (d) OCP curves obtained on Mo electrode after potentiostatic electrolysis at -2.5 V (vs Ag/Ag^+) for 10 s in LiCl-KCl-$PbCl_2$ (2.0 wt.%)-$DyCl_3$ (2.0 wt.%) melt. Temperature: 873 K

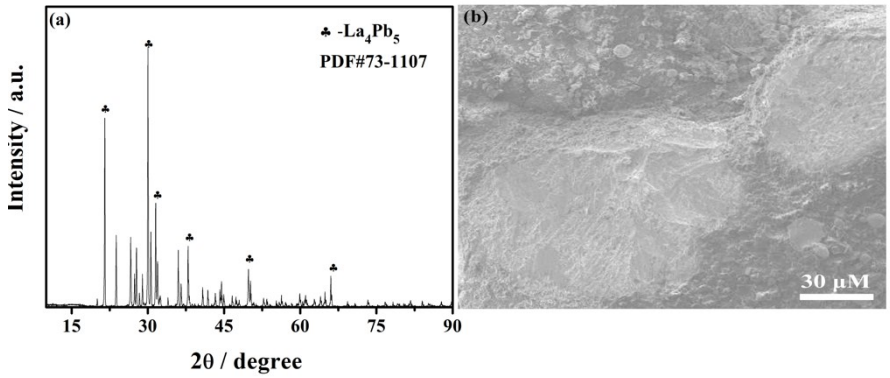

Fig. S6 (a) XRD pattern of deposit obtained by potentiostatic electrolysis at -1.2 V (vs Ag/Ag^+) on molybdenum electrodes for 2 h at 873 K. (b) SEM analysis of the Pb-La alloys.

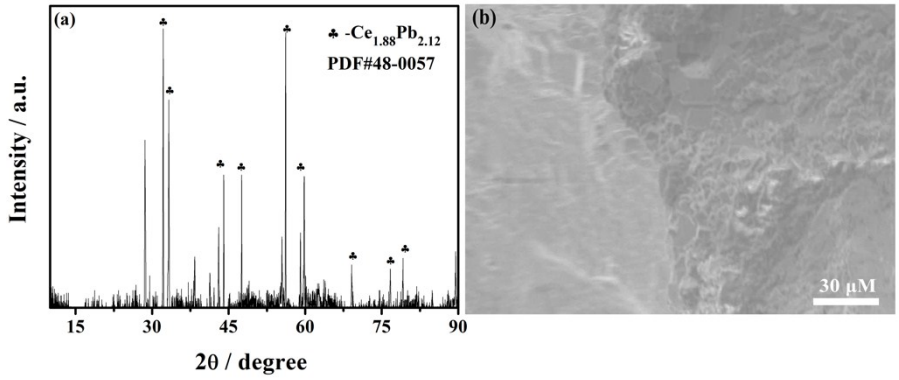

Fig. S7 (a) XRD pattern of deposit obtained by potentiostatic electrolysis at -1.30 V (vs Ag/Ag^{+}) on molybdenum electrodes for 2 h at 873 K. (b) SEM analysis of the Pb-Ce alloys.

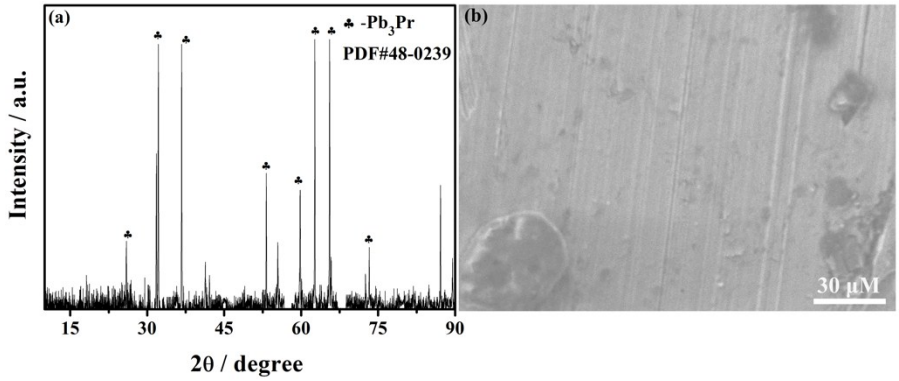

Fig. S8 (a) XRD pattern of deposit obtained by potentiostatic electrolysis at -1.30 V (vs Ag/Ag^{+}) on molybdenum electrodes for 2 h at 873 K. (b) SEM analysis of the Pb-Pr alloys.

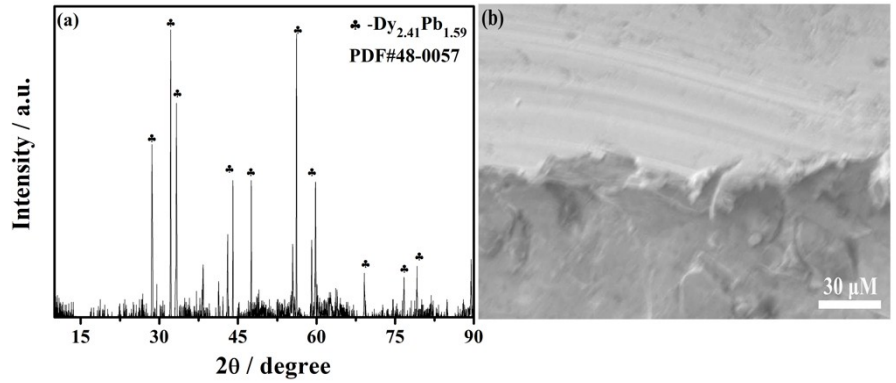

Fig. S9 (a) XRD pattern of deposit obtained by potentiostatic electrolysis at -1.40 V (vs Ag/Ag^{+}) on molybdenum electrodes for 2 h at 873 K. (b) SEM analysis of the Pb-Dy alloys.

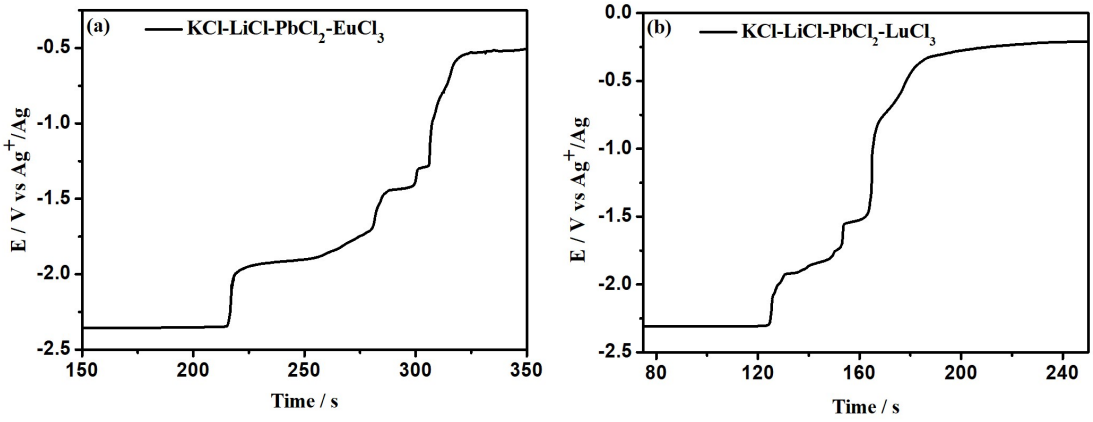

Fig. S10 Open circuit chronopotentiometry curves obtained on a Mo electrode at 873 K after potentiostatic electrolysis at -2.5 V (vs Ag/Ag^{+}) for 10 s in LiCl-KCl-$PbCl_2$ (2.0 wt.%)-$EuCl_3$ (2.0 wt.%) melt (a), LiCl-KCl-$PbCl_2$ (2.0 wt.%)-$LuCl_3$ (2.0 wt.%) melt (b).

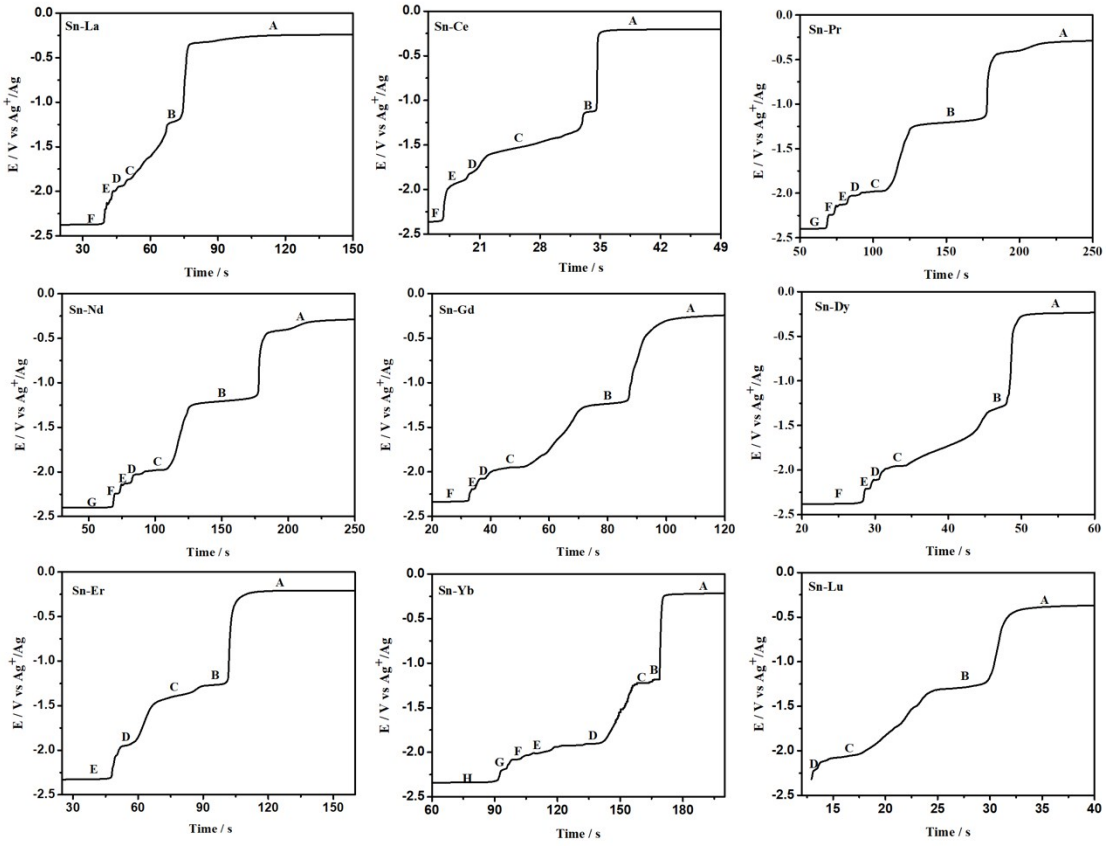

Fig. S11 Open circuit chronopotentiometry curves obtained on a Mo electrode at 873 K after potentiostatic electrolysis at -2.5 V (vs Ag/Ag^{+}) for 10 s in LiCl-KCl-$SnCl_2$ (2.0 wt.%)-$LnCl_3$ (2.0 wt.%) melt (Ln include La, Ce, Pr, Nd, Gd, Dy, Er, Yb and Lu).

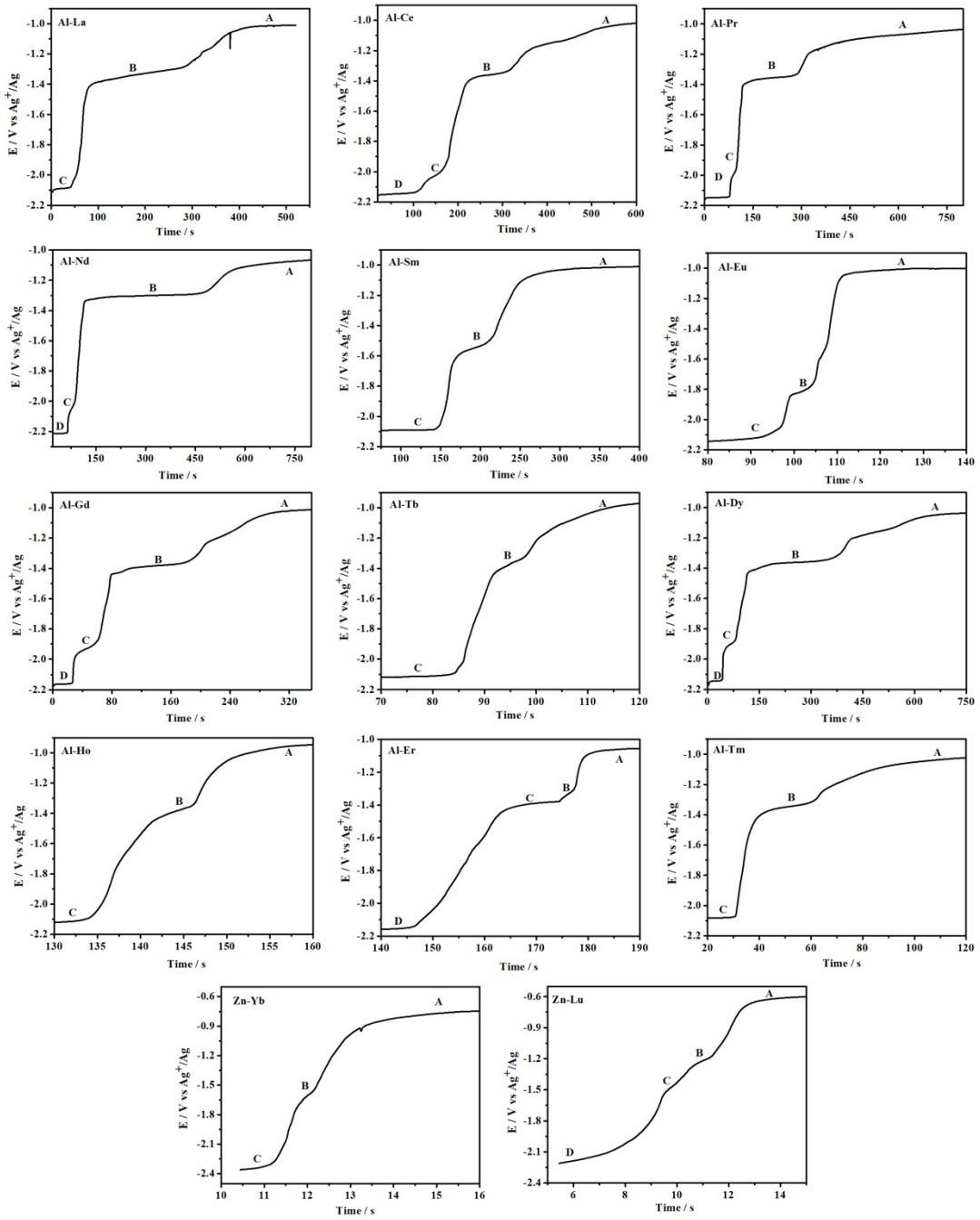

Fig. S12 Open circuit chronopotentiometry curves obtained on a Mo electrode at 873 K after potentiostatic electrolysis at -2.5 V (vs Ag/Ag^+) for 10 s in LiCl-KCl-$AlCl_3$ (2.0 wt.%)-$LnCl_3$ (2.0 wt.%) melt (Ln include La-Lu).